

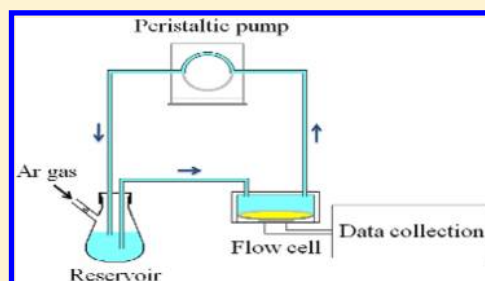
# Quartz Crystal Microbalance (QCM): Useful for Developing Procedures for Immobilization of Proteins on Solid Surfaces

Xue Sha,<sup>†</sup> Chengjun Sun,<sup>†,§</sup> Xiaohe Xu,<sup>†</sup> Laura Alexander,<sup>‡</sup> Patrick J. Loll,<sup>‡</sup> and Lynn S. Penn<sup>\*,†</sup>

<sup>†</sup>Department of Chemistry, Drexel University, Philadelphia, Pennsylvania 19104, United States

<sup>‡</sup>Department of Biochemistry and Molecular Biology, Drexel College of Medicine, Philadelphia, Pennsylvania 19102, United States

**ABSTRACT:** We demonstrate the combined use of liquid and air measurements with the quartz crystal microbalance (QCM) for quantitative analysis of multistep reaction procedures leading to immobilized proteins on solid surfaces. Reactions are conducted on the surfaces of QCM sensor crystals and are quantified by measurements of resonant frequency of the crystals before and after each reaction step. When reactions are conducted in the flow cell in the presence of solvent, measurement of resonant frequency can be made in situ (liquid measurement). When reactions cannot be conducted in the flow cell because of temperatures or solvents not tolerated by the cell, frequency can be measured after evaporation of solvent (air measurement). Each reaction step can be analyzed by either liquid or air measurement so that the whole multistep procedure is addressed, no matter how diverse the chemical nature of the steps. We conducted identical multistep procedures on two different starting surfaces, gold and silica, and found comparable results.



## INTRODUCTION

Researchers immobilize proteins on solid surfaces for a variety of applications, including medical diagnostic devices, drug development studies, drug delivery, etc. Typically, diverse requirements are met by conducting preliminary reactions on the surface prior to attachment of the protein itself, necessitating a multistep procedure. The chief problem is that individual steps are difficult to quantify, because the relatively thin layer formed by each reaction step contains an insufficient volume of material for most analytical methods. This problem underlies numerous reports in the literature that lack quantitative, and even semiquantitative, characterization of multistep immobilization procedures. The quartz crystal microbalance (QCM) has the potential to overcome this problem, because it is a highly surface-sensitive technique that can quantify each successive step of a multistep surface modification procedure.

The heart of the QCM is a piezoelectric quartz crystal in the shape of a thin disk. This crystal, situated in a flow cell as shown in Figure 1, is the sensing element of the system and is integrated into an electrical circuit. Several times per second, the crystal is set into free vibration (in-plane shear) by a pulse of current; each time the vibration dies out naturally. As material from the passing solution is deposited on, or coupled to, the surface of the crystal sensing element, the instrument records the changes in both resonant frequency and energy dissipation of the vibrating crystal. The instrument reports  $\Delta f_n/n$  in hertz, where  $n$  is the vibrational mode number and  $\Delta f_n$  is the frequency change for mode  $n$ . It also reports  $\Delta D$ , the ratio of dissipated energy to stored energy per cycle of vibration of the sensor crystal. This ratio is unitless and of order of magnitude  $10^{-6}$ .

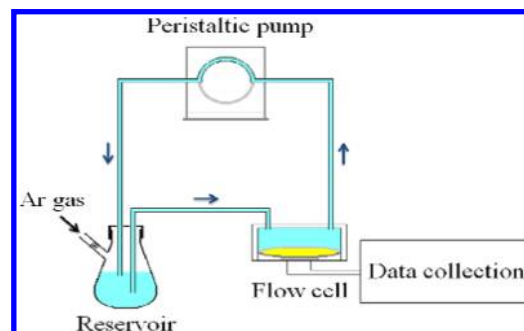


**Figure 1.** Circulation system of QCM system for real-time monitoring of reactions on the surface of the sensor crystal inside the flow cell, with flowing liquid in cyan and crystal disk in yellow. The figure exaggerates the relative size of the flow cell; the disk is 14 mm in diameter, and the liquid volume above the disk is 40  $\mu\text{L}$ .

If the layer deposited from solution is ultrathin and elastic, then the energy dissipation is negligible and the frequency change is directly proportional to mass deposited, according to the Sauerbrey equation,<sup>1–3</sup>

$$\Delta m = -C \frac{\Delta f_n}{n}$$

where  $\Delta m$  is the mass change,  $C$  is an instrument constant, and  $n$  and  $\Delta f_n$  are as defined previously. If the deposited layer is thick, and especially if it contains entrained solvent, it will be viscoelastic and show considerable energy dissipation during

**Received:** August 8, 2012

**Accepted:** November 5, 2012

**Published:** November 5, 2012

vibration. Consequently, the decrease in frequency is *greater* for a viscoelastic layer than for a perfectly elastic layer, and the Sauerbrey equation yields an overestimate of the actual mass of the nonsolvent material in the layer.<sup>4–11</sup> However, evaporation of the solvent from the viscoelastic layer will allow it to collapse into a thin, elastic layer of negligible dissipation, to which the Sauerbrey equation can be applied to yield an accurate value for mass per unit area. The latter approach is valuable not only when the solvated layer is viscoelastic but also when conditions of a particular reaction step prevent it from being conducted in the flow cell at all.

Elastic layers can be distinguished from viscoelastic layers by means of two features of the QCM data. For a thin, elastic layer, the frequency data,  $\Delta f_n/n$ , for multiple vibrational modes will be superimposed (typically several vibrational modes are monitored) and  $\Delta D$  will be negligible, e.g., less than  $2 \times 10^{-6}$  (critical value is discussed in a later section). By contrast, for a viscoelastic layer, the frequency data,  $\Delta f_n/n$ , will have different values for different vibrational modes and the value for  $\Delta D$  will not be negligible. These features can tell the experimenter whether or not evaporation of solvent and measurement of the collapsed layer in air is required.

The present paper describes the combination of the more usual use of the QCM, to analyze layers in the flow cell in the presence of solvent, with the use of *the same instrument* to analyze layers from which the solvent has been evaporated. This combined use of liquid and air measurements permits all of the steps of a multistep procedure to be analyzed quantitatively. Two different solid surfaces were used: gold, a popular starting surface for laboratory studies involving the immobilization of protein, and silica, a nonmetal that can be used in applications that cannot tolerate the presence of a metal. In brief, the steps were (1) introduction of reactive groups to the solid surface (if necessary), (2) grafting of polyethylene glycol (PEG) chains to the solid surface, (3) attachment of protected cysteines to the free ends of the PEG chains, (4) deprotection of the amine groups of the cysteines, (5) deprotection of the thiol groups of the cysteines, and (6) attachment of protein thioesters to the cysteine residues by covalent bonding. The process is summarized in Figure 2, where the starting surface is silica.

The purpose of grafting poly(ethylene glycol), or PEG, chains to the solid surface is to prevent nonspecific adsorption of protein and to provide spacers separating the protein from the underlying surface. The mechanism by which grafted PEG prevents protein from reaching and adsorbing to the underlying solid surface has been the subject of many studies in recent years.<sup>12–24</sup> There is considerable evidence that the two most important features for PEG chains are conformational mobility and hydration, i.e., the free length of each grafted chain must be mobile and must carry layers of entrained water. A grafted layer of chains can have two conformations—mushroom and brush. In a mushroom layer, the chains are not crowded and each chain assumes a hemispherical shape analogous to its spherical conformation in solution. In a brush, the grafted chains are crowded and, as a result, are contracted laterally and extended vertically, away from the surface to avoid mutual overlap. Grafted PEG chains in either the mushroom or brush conformation meet the requirements of mobility and hydration, because both conformations are  $\sim 90\%$  water and  $\sim 10\%$  polymer by volume and both types act as barriers to penetration by larger molecules. We used heterobifunctional PEG chains terminating at one end with a thiol group and at the other end with a primary amine group, selecting the thiol

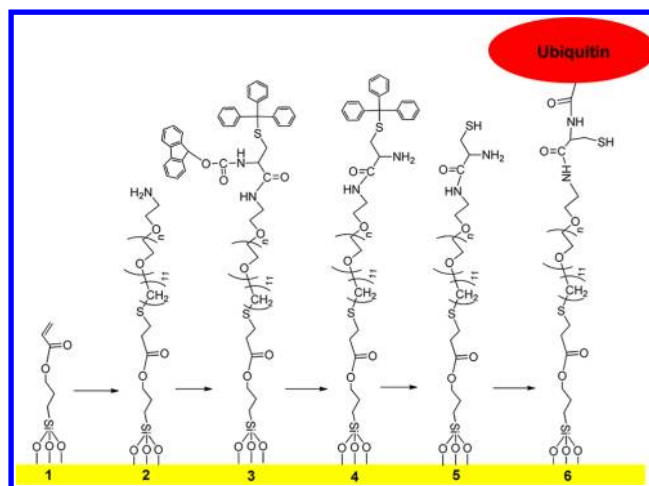


**Figure 2.** Steps leading to immobilization of protein to the surface of a sensor crystal. (1) Derivatization of silica surface with acryloxy functional groups, (2) grafting of  $\alpha$ -thioalkyl- $\omega$ -amino PEG chains, (3) coupling of protected cysteines to free ends of PEG chains, (4) removal of protecting groups from amine of the cysteines, (5) removal of protecting groups from thiol of the cysteines, and (6) chemical bonding of ubiquitin thioesters to cysteine residues.

group for its ability to form a strong bond with both the untreated gold surface and the acryloxy-derivatized silica surface. We intended the primary amine group to remain free to react with protected cysteine in the next step.

The purpose of coupling protected cysteine to the free amine ends of the grafted PEG chains was to have the chains terminate in cysteine residues that could participate after deprotection in native chemical ligation. Native chemical ligation is an alternative to the more traditional immobilization involving formation of a coordination bond between a hexahistidine tag on the protein and a nickel complex previously attached to a solid surface.<sup>25–28</sup> The bond based on a hexahistidine tag can be broken easily by the mechanical shearing action of flowing liquid,<sup>27</sup> a major drawback in many applications. Native chemical ligation, on the other hand, results in a peptide bond (covalent) between the cysteine residue and the thioester-modified C-terminus of a protein.<sup>29–32</sup> For this ligation, the C-terminus of the protein must carry a thioester group, which undergoes a trans-thioesterification reaction with the  $-\text{SH}$  of the cysteine residue. Then, an N-acyl rearrangement takes place spontaneously to form the peptide bond.

In conducting the planned multistep surface modification, our hypothesis was that the combined use of liquid and air measurements with the quartz crystal microbalance would be able to provide quantitative information about the yields of all of the steps.

## EXPERIMENTAL PROCEDURES

**Quartz Crystal Microbalance.** A quartz crystal microbalance with dissipation monitoring, model E4 QCM-D from Q-Sense Inc. (Gothenburg, Sweden), was used. The sensing element of this instrument was an AT-cut piezoelectric quartz disk with a diameter of 14.0 mm, a thickness of 0.3 mm, a resonant frequency of 4.95 MHz, and a total sensing area of  $154 \times 10^{12} \text{ nm}^2$ . One side of each sensor crystal bore a 50-nm thick layer of either gold or amorphous deposited  $\text{SiO}_2$ , while the other side bore a deposited metal electrode. Prior to use or

reuse, all crystals were exposed to UV-ozone (Procleaner, Bioforce Nanosciences) treatment for 15–30 min to remove any organic matter from the surface. The temperature of the flow cells was controllable in the range 10–40 °C to a precision of 0.02 °C. A peristaltic pump drew solvents and solutions from the reservoir through the flow cells at a rate of 88  $\mu\text{L}/\text{min}$ . Liquid volume above the sensor crystal was 40  $\mu\text{L}$ . For reaction steps conducted in the flow cell, continuous measurements of  $\Delta f_n/n$  (in Hz) and  $\Delta D$  (no units) for three vibrational modes ( $n = 3, 5,$  and  $7$ ) were made in the flowing liquid on at least three replicate crystals. Before each reaction step, the instrument was zeroed and a new stable baseline was established. For reaction steps conducted in other reaction vessels and not in the flow cells, the solvent was evaporated after completion of the reaction, each crystal was rinsed, dried, seated in the empty flow cell, and measurements of  $\Delta f_n/n$  and  $\Delta D$  for three vibrational modes ( $n = 3, 5,$  and  $7$ ) were made in air, before and after reaction, on at least three replicate crystals. The measurements made in air had an inherently larger random error than those made in flowing liquid, because the former required seating and clamping of the crystal both before and after reaction, whereas the latter required seating and clamping only once, i.e., prior to reaction. In the present paper, we use the term “residual” frequency (or dissipation) when referring to the difference in  $\Delta f_n/n$  (or  $\Delta D$ ) before and after a reaction step, regardless of whether it was conducted in liquid or air.

**Contact Angle Measurements.** The advancing contact angles of sessile drops of water were measured with a custom-made goniometer. Droplets of deionized water (each 1.0  $\mu\text{L}$  from a micropipet) were placed on the surface of interest to produce the advancing contact angle. Two measurements were taken from each of four droplets, and the contact angles were reported as the average  $\pm$  one standard deviation.

**Derivatization of Silica Sensor Crystals with Organofunctional Silane.** Temperatures higher than 40 °C were required for this reaction, so it could not be conducted in the flow cells of the QCM. Instead, it was conducted on a Schlenk line, under anhydrous conditions. A Teflon holder containing silica sensor crystals was placed in a 100-mL flask, which was evacuated and refilled with argon three times successively before freshly distilled toluene ( $\sim 30$  mL) and 0.10 mL of organofunctional silane (acryloxypropyl trimethoxysilane) were added with a syringe. The contents of the flask were heated to  $70 \pm 2$  °C for 48 h under argon, after which the sensor crystals were removed and washed three times in toluene with sonication. The acryloxy-derivatized crystals were dried with flowing argon, subjected to contact angle measurement, and stored in a desiccator until needed.

**Evaluation of Solvents.** To ensure that the residual frequency (difference measured before and after the reaction step) was due solely to chemically bonded species, solvents used in reaction steps had to be able to prevent the irreversible adsorption of reagents not chemically bonded to the sensor surface. Therefore, all prospective solvents and solvent mixtures were evaluated for their ability to sweep all nonchemically bonded solutes from the surface of the crystal. An extensive series of tests was conducted, including bare surfaces, surfaces treated to be nonreactive under the prevailing conditions (e.g., *n*-propyl-derivatized silica), and solutes in versions not reactive with the surface under the prevailing conditions (e.g., ubiquitin without the thioester end group and  $\alpha$ -hydroxy- $\omega$ -methoxy PEG of the same molecular weight as the  $\alpha$ -amino- $\omega$ -thiol PEG used for grafting). To qualify for use in any of the reactions

steps, a solvent had to show behavior as shown in Figure 3; introduction of pure solvent to the flow cell to establish

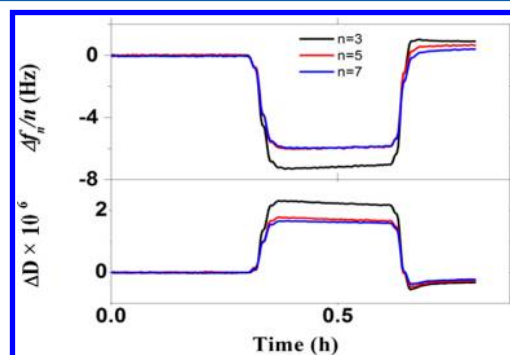


**Figure 3.** QCM responses for sequence of pure dimethyl formamide, solution of piperidine in dimethyl formamide, and again pure dimethyl formamide through the flow cell. The change from pure solvent to solution produces the small but observable drop in  $\Delta f_n/n$  (and increase in  $\Delta D$ ) at  $\sim 0.3$  h. Responses revert to original values upon reintroduction of the pure solvent at  $\sim 0.65$  h, verifying the ability of the solvent to remove all nonchemically bonded species from the sensor crystal.

baselines for  $\Delta f_n/n$  and  $\Delta D$ , introduction of a solution of reactant/reagent in the same solvent showing a small shift in  $\Delta f_n/n$  and  $\Delta D$ , and reintroduction of pure solvent producing a return of  $\Delta f_n/n$  and  $\Delta D$  to the baselines. An incomplete return of  $\Delta f_n/n$  and  $\Delta D$  to the baseline was taken to indicate inability of the solvent to prevent irreversible adsorption of reagent to the sensor surface, and the solvent was disqualified from further use.

**Model Michael Reactions in Solution.** Michael reactions between small thiol molecules and the double bond of an acryloxy group were conducted in solution to assess the effect of different amine catalysts on percent yield. For each reaction, a 25-mL flask was evacuated and refilled with argon three times. Freshly distilled toluene ( $\sim 7$  mL), acryloxy propyl trimethoxysilane (0.470 g, 2.01 mmol), 1-hexanethiol (0.289 g, 2.44 mmol), and either 800  $\mu\text{L}$  of *N,N*-di-isopropyl ethylamine, 17  $\mu\text{L}$  of ethylene diamine, or 26  $\mu\text{L}$  of diethyl amine were added to the flask. The reaction mixtures were stirred overnight at room temperature. Proton magnetic resonance was used to follow the disappearance of the peaks characteristic of the three alkene protons (chemical shifts of three multiplets centered at 5.9, 6.3, and 6.5 ppm downfield from the internal reference compound) of the acryloxy propyl trimethoxysilane as 1-hexanethiol reacted with it. Spectra showed that model reactions catalyzed by the primary and secondary amines, ethylenediamine and diethylamine, went to completion (alkene peaks disappeared completely), while the model reaction catalyzed by the tertiary amine, *N,N*-diisopropylethylamine, went to 60–70% completion. An explanation for the difference is that the primary and secondary amines act as nucleophilic agents, while tertiary amine acts merely as a simple base.<sup>33</sup> Of the two catalysts that gave 100% yield, ethylene diamine was selected arbitrarily for further use in reactions conducted in the QCM.

**Grafting of Polyethylene Glycol to Silica.** For this step, HS-PEG-NH<sub>2</sub>, or  $\alpha$ -amino- $\omega$ -thiol PEG, of  $M_n = 2400$  g/mol and  $M_w/M_n = 1.2$  (verified by matrix-assisted laser desorption ionization mass spectrometry) was used. The complete end-groups were undecylthiol and amine, respectively (Polymer

Source, Dorval, Canada). Because the Michael reaction to graft HS-PEG-NH<sub>2</sub> to the acryloxy-derivatized sensor surfaces went too slowly to be practical at temperatures within the capability of the flow cell, it was conducted at elevated temperature, i.e., 70 ± 2 °C, well above the 40 °C maximum of the flow cell. For this, HS-PEG-NH<sub>2</sub> (17.9 mg, 0.00746 mmol) was added as a dry powder to a 50-mL flask. A Teflon holder containing acryloxy-derivatized sensor crystals was then placed in the flask. The flask was attached to a Schlenk line and was evacuated and refilled with argon three times, after which freshly distilled toluene (~20 mL) and ethylene diamine catalyst (5.0 μL) were added with a syringe. Once the solids had dissolved completely, the reaction was permitted to proceed at 70 ± 2 °C for 72 h under argon. After reaction, the sensor crystals were rinsed sequentially with toluene and ethanol in a sonicator, were dried under flowing argon, and were stored in a desiccator until the next step.

**Grafting of Polyethylene Glycol to Gold.** Grafting of polyethylene glycol to gold was conducted in the QCM at room temperature (20 ± 0.02 °C). Bare gold sensor crystals were seated in the flow cells of QCM, and a mixed solvent composed of ethanol:water (1:5 by volume) was drawn through the cells until a stable baseline was established. Then a solution of HS-PEG-NH<sub>2</sub> (30.0 mg, 0.0125 mmol) in ~20 mL of the same mixed solvent was sonicated to remove air bubbles and was recycled through the flow cells for 4 h at room temperature to allow the grafting of HS-PEG-NH<sub>2</sub> to the gold surface. After this, the same mixed solvent was reintroduced and was drawn through the flow cells to waste for 1–2 h to rinse away any nonchemically bonded species. The sensor crystals were dried under flowing argon and were stored in a desiccator until the next step.

**Coupling of Protected Cysteine to the Amine Ended-PEG.** The coupling of protected cysteine was conducted in the flow cells of the QCM. The cysteine was purchased with its thiol and primary amine groups protected with triphenyl methyl (Trt) and 9-fluorenylmethyloxycarbonyl (Fmoc) groups, respectively, leaving the carboxylic acid group free to react with the amine ends of the grafted PEG chains. Fmoc was selected over the more common benzyloxy carbonyl (Boc) protecting group because the former could be removed with relatively mild conditions, while removal of Boc required conditions that damaged the gaskets of the QCM flow cells. The same coupling procedure was used for both derivatized silica and gold solid surfaces. The sensor crystals bearing grafted PEG chains were seated in the flow cells of the QCM, and freshly distilled DMF was recycled through the cells until a stable baseline was established. In the meantime, the solution of reagents for the coupling reaction was prepared on the Schlenk line. Preparing this solution consisted of weighing the following dry reagents and adding them to a 50-mL flask: protected cysteine (62.5 mg, 1.07 × 10<sup>-4</sup> mol) and activating reagent HBTU (38 mg, 1.0 × 10<sup>-4</sup> mol). The flask containing the dry solids was attached to the Schlenk line and was evacuated and refilled with argon three times. Freshly distilled DMF (30 mL) was added with a syringe to the solids, and the mixture was stirred until all solids were dissolved. Last, DIPEA (50 μL, 37 mg, 2.9 × 10<sup>-4</sup> mol) was added with a syringe, and the solution was stirred. The flask containing the solution was removed from the Schlenk line, sonicated to remove air bubbles, and recycled through the flow cells for 4 h at room temperature (20 ± 0.02 °C). After this, freshly distilled DMF was drawn through the flow cells to waste to rinse away any nonchemically bonded

species. After 1–2 h of rinsing, the sensor crystals were allowed to remain in the flow cells for the deprotection steps, described next.

**Deprotection of the Cysteine Residue.** The protected amine and thiol groups of the cysteine coupled to the grafted PEG chains were deprotected in separate steps. For removal of the Fmoc protecting group from the cysteine amine group, freshly distilled DMF was drawn through the flow cells containing the sensor crystals until a stable baseline was established. Then a solution of piperidine (4.0 mL) in freshly distilled DMF (16 mL) was recycled through the flow cells for 2 h. After this, freshly distilled DMF was drawn through the flow cells to waste to rinse the crystals. Crystals having underlying gold surfaces were subjected to an extra treatment: an exposure to mercapto-undecanol to block any exposed patches of gold and render them unreactive to the thiol groups uncovered in the next deprotection step.

For removal of the Trt protecting group from the cysteine thiols, a stable baseline was established with freshly distilled CH<sub>2</sub>Cl<sub>2</sub>. Then a solution of TFA (2.0 mL) and triisopropylsilane (1.0 mL) in freshly distilled CH<sub>2</sub>Cl<sub>2</sub> (17 mL) was recycled through the flow cells. After 1 h, the recycling solution was replaced with freshly distilled CH<sub>2</sub>Cl<sub>2</sub> drawn through the cells to waste to rinse the crystals for 1–2 h.

**Preparation of Ubiquitin Thioester.** *E. coli* cells (Rosetta (DE3), Novagen/EMD4Biosciences) were transformed with a plasmid encoding ubiquitin residues 1–75 fused to a His<sub>6</sub>-tagged *Mycobacterium xenopi* intein.<sup>34</sup> Cultures of 1 L were grown at 24 °C for 24 h in self-inducing media,<sup>35</sup> after which the cells were pelleted and resuspended in 50 mL of Buffer A (50 mM sodium phosphate pH 7.4, 250 mM NaCl, 7.5 mM imidazole, 10 mM magnesium sulfate, 2 μg/mL each RNase and DNase). The cells were lysed by two passes through an Emulsiflex C5 homogenizer (Avestin, Inc.), and the lysate was centrifuged at 30 000g for 30 min to remove cell debris. The supernatant was applied to two 5-mL immobilized-metal affinity columns (HiTrap IMAC HP, GE Life Science), connected in series and pre-equilibrated with Buffer A. After exhaustive washing with Buffer A + 0.1% Triton-X100, the ubiquitin-intein fusion protein was eluted with 25 mM sodium acetate pH 3.6, 250 mM NaCl; the protein was eluted into tubes containing sufficient HEPES buffer to bring the fractions' pH to approximately 8. Protein-containing fractions were pooled, and the protein concentration adjusted to 0.2 mM by the addition of buffer, after which sodium 2-mercaptoethanesulfonate (MESNA, 500 mM) and EDTA (200 mM) were added. This reaction mixture was incubated overnight at room temperature and subsequently dialyzed against 25 mM 2-mercaptoethanesulfonic acid (MES) pH 6.5, 250 mM NaCl. Subtractive purification using the IMAC HP column then served to remove intein and any uncleaved fusion protein, yielding the desired ubiquitin thioester. The thioester was dialyzed against 20 mM MES pH 6.2 plus 50 mM NaCl, concentrated to 48 mg/mL (~5.6 mM), flash-frozen, and stored at -80 °C.

**Native Chemical Ligation of Ubiquitin Thioester.** Two solutions were prepared in advance of the actual ligation reaction. The first was HEPES (4-(2-hydroxyethyl)-1-piperazine ethanesulfonic acid) buffer, containing 0.10 M sodium HEPES (pH 8.0) and 0.50 NaCl. The second was ~63 mM 4-mercaptophenylacetic acid (MPAA), prepared by mixing MPAA (42.7 mg, 0.254 mmol) with 4.0 mL of HEPES buffer in a 10-mL vial. This mixture was sonicated to promote

**Table 1. Predicted Frequencies (Sauerbrey Equation), Measured Residual Frequencies, and Measured Residual Dissipations for Reactants Added to Sensor Surface<sup>a</sup>**

molecule	MW, g/mol	no./nm <sup>2</sup>	g/nm <sup>2</sup>	predicted $\Delta f_n/n$ , Hz	measured $\Delta f_n/n$ , Hz	measured $\Delta D$ , 10 <sup>-6</sup>
acryloxy propyl silane	234	2	$77 \times 10^{-23}$	-4	$-13 \pm 9^*$	$\sim 0^*$
acryloxy propyl silane	234	3	$117 \times 10^{-23}$	-6.6		
HS-PEG-NH <sub>2</sub>	2400	3	$1196 \times 10^{-23}$	-67.6	$-36 \pm 10^*$ for gold;	$\sim 0^*$ for gold;
HS-PEG-NH <sub>2</sub>	2400	1	$399 \times 10^{-23}$	-22.5		
HS-PEG-NH <sub>2</sub>	2400	0.5	$199 \times 10^{-23}$	-11.2	$-45 \pm 14^*$ for derivatized silica	$\sim 0^*$ for derivatized silica
HS-PEG-NH <sub>2</sub>	2400	0.1	$39.9 \times 10^{-23}$	-2.25		
protected cysteine	586	3	$292 \times 10^{-23}$	-16.5	$-3.6 \pm 1.3$ for gold;	$1.0 \pm 0.4$ for gold;
protected cysteine	586	1	$97.3 \times 10^{-23}$	-5.5		
protected cysteine	586	0.5	$48.7 \times 10^{-23}$	-2.75	$0 \pm 2$ for derivatized silica	$0 \pm 1$ for derivatized silica
protected cysteine	586	0.1	$9.73 \times 10^{-23}$	-0.55		
ubiquitin (residues 1-75)	8508	3	$4240 \times 10^{-23}$	-239	$-37 \pm 3$ for gold;	$2 \pm 2$ for gold;
ubiquitin (residues 1-75)	8508	1	$1413 \times 10^{-23}$	-80		
ubiquitin (residues 1-75)	8508	0.5	$707 \times 10^{-23}$	-40	$-25 \pm 5$ for derivatized silica	$2 \pm 1$ for derivatized silica
ubiquitin (residues 1-75)	8508	0.1	$141 \times 10^{-23}$	-8		

<sup>a</sup>\* indicates measurements of the solventless layer in air.

dissolution, and the pH was readjusted to 8.0 with 2.0 M NaOH. Just before use, the solution was passed through a filter membrane (Anodisc 13, 0.02-mm pore size) to remove particulates. For the actual native chemical ligation step, a 50- $\mu$ L aliquot of the buffered ubiquitin thioester solution was thawed. A sensor crystal ready for native chemical ligation was placed in the flow cell, and HEPES buffer was recycled through the flow cells until a stable baseline was obtained. Then, the 50- $\mu$ L aliquot of thawed, buffered 5.6-mM ubiquitin thioester solution was added to 150  $\mu$ L of the buffered MPAA solution. The resultant solution, containing the ubiquitin thioester at pH 8, was introduced to the flow cell at a flow rate of 0.4  $\mu$ L/min, the lowest rate available from the pump, to maximize the contact time of the buffered ubiquitin solution with the sensor crystal. At this flow rate, consumption of the reservoir of ubiquitin solution took approximately 5 h, after which HEPES buffer was drawn through the flow cell to waste for 2–3 h to rinse away unreacted ubiquitin.

## RESULTS AND DISCUSSION

To estimate the expected surface attachment densities for each reaction step in the multistep procedure for the immobilization of protein, it is useful to first consider the desired final result, a two-dimensional monolayer of protein. The ideal monolayer should contain as many protein molecules as possible without requiring that they deform to fit. Obviously, this number is dependent on the size of the protein molecules. Ubiquitin, the test protein in the present study, has a hydrodynamic radius of  $\sim 1.3$  nm,<sup>36–38</sup> corresponding to a cross-sectional area of 5.3 nm<sup>2</sup>. Therefore, a well-packed monolayer of ubiquitin is predicted to consist of  $\sim 0.19$  molecules/nm<sup>2</sup>, and the yields of the preceding reaction steps must be high enough for this value to be achieved.

It is important that the bare surfaces used as starting materials in this study have a sufficient number of active sites to allow grafting of PEG chains at a density in excess of 0.19 chains/nm<sup>2</sup>. Fortunately, both gold and silica have more than sufficient density of reactive sites. The gold surface, for which each trio of atoms is considered an active site, has  $\sim 5$  reactive sites per nm<sup>2</sup>. The silica surface contains about 5–6 native hydroxyl groups per square nanometer,<sup>39,40</sup> which can be converted upon derivatization with commercially available organofunctional silanes to  $\sim 3$  reactive sites per square

nanometer.<sup>41</sup> Thus, both surfaces provide more than enough sites for grafting of an excess of PEG chains.

As stated in the introduction, to minimize nonspecific adsorption of protein to the underlying surface, the grafted PEG chains can be in the form of either a mushroom layer or a brush. In a mushroom layer, each hemispherically shaped grafted chain surmounts a circular area on the grafting surface equal to  $\pi R^2$ , where  $R$ , the radius of gyration expanded by the swelling due to solvent–polymer interactions, is a measure of hydrodynamic radius.<sup>42</sup> For the polyethylene glycol chains used in the present work,  $M_n = 2400$  g/mol and  $R = 1.7$  nm in toluene. This means that each chain in a mushroom layer covers 9.1 nm<sup>2</sup> of surface area and that the surface attachment density is  $\sim 0.10$  chains/nm<sup>2</sup>. This surface attachment density is not sufficient to accommodate the immobilization of 0.19 ubiquitin molecules/nm<sup>2</sup>. In a brush, where the chains are contracted laterally and extended vertically, the surface attachment density is several times larger. Thus, for immobilization of a monolayer of ubiquitin, a brush is required.

For each step in the multistep procedure, the residual  $\Delta f_n/n$  (difference before and after reaction) provides a measure of the amount of material added to the sensor surface by the chemical reaction. Table 1, which can be referred to in the remainder of the discussion, shows predicted residual frequencies, computed from the Sauerbrey equation, for different surface attachment densities of the reactant used in each step. Also shown in Table 1 are the experimentally measured residual  $\Delta f_n/n$  and  $\Delta D$  for each reaction step. The values listed in the table are from liquid measurements, made in the QCM in the presence of solvent, unless marked by an asterisk. Those so marked are values from measurements in air, performed after evaporation of the solvent. For the Sauerbrey equation to compute an accurate value for the mass of the added layer, the residual dissipation must be negligible. The problem is that no absolute criterion exists to establish dissipation as negligible. In the absence of an absolute criterion, an often-used rule of thumb is that the Sauerbrey equation gives a correct value for mass added if the  $\Delta D$  value associated with the layer is  $\leq 2 \times 10^{-6}$ .<sup>4</sup> Another practical criterion is that the Sauerbrey equation gives the correct mass when the value of  $\Delta D$  multiplied by 10<sup>6</sup> is equal to or less than 5% of the value of  $\Delta f_n/n$  in hertz.<sup>43</sup> In cases when both  $\Delta D \times 10^6$  (unitless) and  $\Delta f_n/n$  (in Hz) are very small and

similar in value, these rules do not apply. All the values reported in Table 1 either meet these criteria or are on the borderline.

The derivatization of the silica surface with acryloxypropyl silane required elevated temperature and therefore was not conducted in the QCM. The advancing contact angle of water changed from  $10 \pm 4^\circ$  on bare silica to  $65 \pm 3^\circ$  on acryloxy-derivatized silica, indicating a change from extremely hydrophilic to moderately hydrophobic, as expected from the surface chemistry. Results of QCM measurements in air, shown in Table 1, were  $\Delta f_n/n = -13 \pm 9$  Hz, which corresponds to  $5.7 \pm 4.3$  groups/nm<sup>2</sup>, or about two monolayers. Half of these groups ( $\sim 2\text{--}3/\text{nm}^2$ ) would be available for subsequent reaction at the surface of the top monolayer.

The grafting of heterobifunctional-ended polyethylene glycol (HS-PEG-NH<sub>2</sub>) to acryloxy-derivatized silica sensor crystals also required elevated temperature and therefore was not conducted in the QCM. The thiol end-groups of the PEG chains can undergo addition to the carbon-carbon double bonds of the acryloxy groups. Although this reaction is frequently conducted as a photoinitiated free radical reaction,<sup>44–46</sup> it can also occur as a standard Michael reaction, facilitated by the electron-withdrawing acryloxy group attached to the double bond.<sup>33,47–51</sup> A complicating feature of the grafting of the particular heterobifunctional-ended PEG we selected is that the amine end as well as the thiol end can undergo a Michael reaction with the double bond of the acryloxy group. Therefore, the free end-groups of the grafted chains would be expected to be a mixture of -SH and -NH<sub>2</sub>. The consequence of mixed end groups at the free ends of the grafted chains would be reduction of the yield of the subsequent step—the coupling of protected cysteines to the primary amine groups at the free ends of the grafted PEG chains. This consequence is considered later, in the discussion of immobilization of the protein.

Qualitative verification of the grafting of PEG was provided by the advancing contact angle of water. This changed from  $65 \pm 3^\circ$  before grafting to  $35 \pm 2^\circ$  after grafting, which is a change that is consistent with a moderately hydrophobic surface becoming hydrophilic. To obtain a quantitative value for mass attached, we used the QCM to conduct measurements in air of crystals containing grafted PEG chains from which the solvent had been evaporated. These measurements (Table 1) of collapsed grafted PEG layers yielded a residual frequency of  $-45 \pm 14$  Hz (from three replicate crystals), which corresponds to  $2.0 \pm 0.6$  chains/nm<sup>2</sup>. The zero value of residual dissipation, as well as the superimposed values of  $\Delta f_n/n$  for all  $n$ , confirmed that the dry PEG layers were compact and elastic.

The grafting of functional-ended polyethylene glycol (HS-PEG-NH<sub>2</sub>) to gold was done in the flow cell of the QCM at room temperature ( $20 \pm 0.02$  °C). The average residual frequency,  $\Delta f_n/n$ , obtained in the presence of solvent was  $57 \pm 5$  Hz; the accompanying  $\Delta D$  value was  $5.4 \times 10^{-6} \pm 1.3 \times 10^{-6}$  (unitless). This  $\Delta D$  value is large enough to suggest that the mass computed from the Sauerbrey equation is an overestimate. To obtain an accurate value of the mass of the grafted polymer, we measured the residual frequency in air of the grafted layer of PEG chains. As reported in Table 1, the value obtained for this collapsed layer was  $-36 \pm 10$  Hz (from three replicate crystals), for which the Sauerbrey equation gave a mass corresponding to  $1.6 \pm 0.5$  chains/nm<sup>2</sup>. The average values shown in Table 1 for PEG grafted to gold and PEG grafted to derivatized silica are statistically the same (double-tailed Student  $t$  test,  $0.4 < p < 0.6$ ). In both cases, this surface

attachment density is in excess of that needed for the ultimate immobilization of 0.19 ubiquitins/nm<sup>2</sup>.

The next step, the coupling of protected cysteine to the grafted PEG brush, was conducted in the QCM. The values obtained for residual  $\Delta f_n/n$  and  $\Delta D$  are listed in Table 1. For the PEG brush on gold, the coupling step produced a residual frequency that was small but easily distinguished from the baseline. In cases such as this, when residual  $\Delta f_n/n$  and  $\Delta D$  are both small, dissipation is negligible and the Sauerbrey equation can be applied. The Sauerbrey equation yields 0.65 protected cysteine groups/nm<sup>2</sup> for this step, i.e., a 41% yield for this coupling reaction. By contrast, the QCM data for coupling of protected cysteine to the PEG brush on derivatized silica could not be distinguished from zero when experimental error was taken into consideration and, therefore, were deemed inconclusive. However, coupling in this case was verified by the success of a later step, the native chemical ligation of protein to the layer.

The deprotection steps were also conducted in the QCM flow cell. The deprotection steps gave values for residual  $\Delta f_n/n$  and  $\Delta D$  that were too small to be definitive. This was not unexpected, because even less mass was removed in each deprotection step than was added in the coupling of the protected cysteine to the free ends of the PEG chains.

The last step of the multistep procedure was the native chemical ligation reaction involving the cysteine residue at the end of the grafted PEG chains and the thioester-modified C-terminus of a protein in solution pH 8. This can be slow, because alkylthiols are not good leaving groups. The addition of an arylthiol (MPAA) as a transfer agent enhanced the rate of thioester exchange reaction involving the  $\alpha$ -thioester of the protein and the cysteine residue linked to the solid surface.<sup>52</sup> Native chemical ligation was conducted in the QCM, and an example of experimental data is presented in Figure 4, for gold

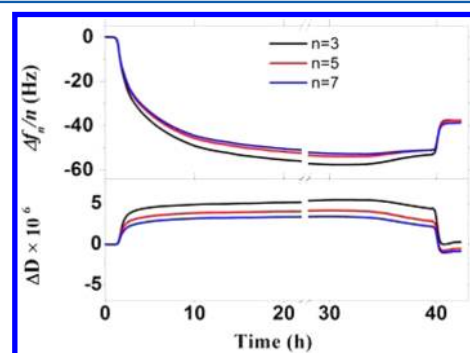


**Figure 4.** QCM traces for native chemical ligation of ubiquitin and cysteine residue. The  $n$  values are the vibrational mode numbers.

as the underlying solid surface. The superposition of the  $\Delta f_n/n$  data for all  $n$  upon rinsing and the return of the  $\Delta D$  value to zero indicates that the layer of protein added in this step is elastic. Control experiments showed that a small amount of apparently adsorbed ubiquitin could be removed from the layer by increasing the flow rate during rinsing, but copious rinsing at higher flow rates produced no further changes. The experimental values of residual  $\Delta f_n/n$  and  $\Delta D$  obtained for this step are listed in Table 1 for both gold and silica as the underlying solid surfaces. The surface attachment densities, corrected for the small amount of adsorbed ubiquitin, were  $0.20 \pm 0.04$  ubiquitin/nm<sup>2</sup> for gold and  $0.10 \pm 0.02$  ubiquitin/nm<sup>2</sup>

for silica. These values compare well with the 0.19 ubiquitin/nm<sup>2</sup> predicted for a monolayer.

The difference between the attachment density for ubiquitin on gold versus on derivatized silica is statistically significant (double tailed student *t* test, 0.02 < *p* < 0.03) and can be attributed to the step in which the HS-PEG-NH<sub>2</sub> was grafted. As previously mentioned, both -SH and -NH<sub>2</sub> are able to undergo the Michael reaction with the double bond of the acryloxy group of the derivatized silica surface, which produces a layer in which some of the grafted PEG chains terminate in -SH and others in -NH<sub>2</sub>. Since the protected cysteine can react only with those PEG chains having free ends of -NH<sub>2</sub>, the observed attachment density of ubiquitin is slightly lower on the silica solid surface than on the gold.

## CONCLUSIONS

We have applied the QCM technique to a multistep reaction procedure designed to immobilize proteins on solid surfaces. Frequency and dissipation measurements can be made in the flow cell in the presence of solvent or in air after evaporation of solvent with the same instrument. If the layer attached in a particular step is ultrathin and elastic, the Sauerbrey equation will provide an accurate conversion of observed frequency change to mass of the layer. However, for liquid measurement of a thick layer, infused with solvent and viscoelastic, use of the Sauerbrey equation to convert frequency change to mass will yield an overestimate of the nonsolvent mass of the layer. In these cases, the solvent can be evaporated to produce a compact, collapsed, and elastic layer, and the frequency changes obtained from measurements made in air provide exact valid values of mass added. For a multistep surface modification, the combination of liquid and air measurements of frequency change provides comprehensive quantitative analysis of the mass attached during the whole procedure. In the present study, the multistep procedure was conducted on two different solid surfaces—gold and silica—with comparable results.

## AUTHOR INFORMATION

### Corresponding Author

\*Mailing address: Department of Chemistry, 305 Disque Hall, Drexel University, 3141 Chestnut Street, Philadelphia, PA 19104, USA. Phone: 1-215-895-4970. E-mail: lynn.s.penn@drexel.edu.

### Present Address

<sup>§</sup>College of Materials and Textile Engineering, Jiaxing University, Jiaxing, 314001, China.

### Notes

The authors declare no competing financial interest.

## ACKNOWLEDGMENTS

The authors thank the Commonwealth Universal Research Enhancement, the National Science Foundation CRIF-MU Grant 0840273, Commonwealth of Pennsylvania, and Drexel University, College of Arts & Sciences, for partial support.

## REFERENCES

- (1) Sauerbrey, G. Z. *Phys. A Hadrons Nuclei* **1959**, *155*, 206–222.
- (2) Ward, M. D.; Buttry, D. A. *Science* **1990**, *249*, 1000–1007.
- (3) Schneider, T. W.; Buttry, D. A. *J. Am. Chem. Soc.* **1993**, *115*, 12391–12397.
- (4) Vogt, B. D.; Lin, E. K.; Wu, W.-L.; White, C. C. *J. Phys. Chem. B* **2004**, *108*, 12685–12690.

- (5) Vogt, B. D.; Soles, C. L.; Lee, H.-J.; Lin, E. K.; Wu, W.-L. *Langmuir* **2004**, *20*, 1453–1458.
- (6) Rodahl, M.; Hook, F.; Krozer, A.; Brzezinski, P.; Kasemo, B. *Rev. Sci. Instrum.* **1995**, *66*, 3924–3930.
- (7) Hook, F.; Rodahl, M.; Brzezinski, P.; Kasemo, B. *Langmuir* **1998**, *14*, 729–734.
- (8) Hook, F.; Kasemo, B.; Nylander, T.; Fant, C.; Sott, K.; Elwing, H. *Anal. Chem.* **2001**, *73*, 5796–5804.
- (9) Hook, F.; Voros, J.; Rodahl, M.; Kurrat, R.; Boni, P.; Ramsden, J. J.; Textor, M.; Spencer, N. D.; Tengvall, P.; Gold, J.; Kasemo, B. *Colloids Surf. B* **2002**, *24*, 155–170.
- (10) Voionova, M. V.; Rodahl, M.; Jonson, M.; Kasemo, B. *Phys. Scr.* **1999**, *59*, 391–396.
- (11) Moya, S. E.; Brown, A. A.; Azzaroni, O.; Huck, W. T. S. *Macromol. Rapid Commun.* **2005**, *26*, 1117–1121.
- (12) Walker, M. L.; Vanderah, D. J.; Rubinson, K. A. *Colloids Surf. B* **2011**, *82*, 450–455.
- (13) Vanderah, D. J.; Vierling, R. J.; Walker, M. L. *Langmuir* **2009**, *25*, 5026–5030.
- (14) Vanderah, D. J.; Walker, M. L.; Rocco, M. A.; Rubinson, K. A. *Langmuir* **2008**, *24*, 826–829.
- (15) Vanderah, D. J.; La, H.; Naff, J.; Silin, V.; Rubinson, K. A. *J. Am. Chem. Soc.* **2004**, *126*, 13639–13641.
- (16) Vanderah, D. J.; Valincius, V. G.; Meuse, C. W. *Langmuir* **2002**, *18*, 4674–4680.
- (17) Ngadi, N.; Abrahamson, J.; Fee, C.; Morison, K. *J. Appl. Sci.* **2010**, *10*, 3343–3348.
- (18) Murthy, R.; Shell, C. E.; Grunlan, M. A. *Biomaterials* **2009**, *30*, 2433–2439.
- (19) Unsworth, L. D.; Sheardown, H.; Brash, J. L. *Langmuir* **2008**, *24*, 1924–1929.
- (20) Unsworth, L. D.; Sheardown, H.; Brash, J. L. *Langmuir* **2005**, *21*, 1036–1041.
- (21) Wagner, V.; Koberstein, J. T.; Bryers, J. D. *Biomaterials* **2004**, *25*, 2247–2263.
- (22) Halperin, A. *Langmuir* **1999**, *15*, 2525–2533.
- (23) Lee, S.-W.; Laibinis, P. E. *Biomaterials* **1998**, *19*, 1669–1675.
- (24) Jeon, S. I.; Lee, J. H.; Andrade, J. D.; De Gennes, P. G. *J. Colloid Interface Sci.* **1991**, *142*, 149–158.
- (25) Fischer, M.; Leech, A. P.; Hubbard, R. E. *Anal. Chem.* **2011**, *83*, 1800–1807.
- (26) Wong, L. S.; Khan, F.; Micklefield, J. *Chem. Rev.* **2009**, *109*, 4025–4053.
- (27) Lee, H.-S.; Contarino, M.; Umashankara, M.; Schön, A.; Freire, E.; Smith, A.; Chaiken, I.; Penn, L. S. *Anal. Bioanal. Chem.* **2010**, *396*, 1143–1152.
- (28) Chaga, G. S. *J. Biochem. Biophys. Methods* **2001**, *49*, 313–34.
- (29) Dawson, P. E.; Muir, T. W.; Clark-Lewis, I.; Kent, S. B. H. *Science* **1994**, *266*, 776–779.
- (30) Dawson, P. E.; Churchill, M. J.; Ghadiri, M. R.; Kent, S. B. H. *J. Am. Chem. Soc.* **1997**, *119*, 4325–4329.
- (31) Dawson, P. E.; Kent, S. B. H. *Annu. Rev. Biochem.* **2000**, *69*, 923–960.
- (32) Mapp, A. K.; Dervan, P. B. *Tetrahedron Lett.* **2000**, *41*, 9451–9454.
- (33) Hoyle, C. E.; Bowman, C. N. *Angew. Chem., Int. Ed.* **2010**, *49*, 1540–1573.
- (34) Economou, N. J.; Nahoum, V.; Weeks, S. D.; Grasty, K. C.; Zentner, I. J.; Townsend, T. M.; Bhuiya, M. W.; Cocklin, S.; Loll, P. J. *J. Am. Chem. Soc.* **2012**, *134*, 4637–4645.
- (35) Studier, F. W. *Protein Expr. Purif.* **2005**, *41*, 207–234.
- (36) Jacob, J.; Krantz, B.; Dothager, R.; Thiagarajan, P.; Sosnick, T. *J. Mol. Biol.* **2004**, *338*, 369–382.
- (37) Larios, E.; Li, J. S.; Schulten, K.; Kihara, H.; Gruebele, M. *J. Mol. Biol.* **2004**, *340*, 115–125.
- (38) Makowski, L.; Gore, D.; Mandava, S.; Minh, D.; Park, S.; Rodi, D.; Fischetti, R. F. *Biopolymers* **2011**, *95*, 531–542.
- (39) Roumeliotis, P.; Unger, K. K. *J. Chromatog., A* **1978**, *149* (0), 211–224.

- (40) Parfitt, G. D. *Pure Appl. Chem.* **1976**, *48*, 415–418.
- (41) Mukherjee-Roy, M.; Kurihara, M.; Penn, L. S. *J. Adhesion Sci. Technol.* **1995**, *9*, 953–969.
- (42) Chanda, M. *Advanced Polymer Chemistry: A Problem Solving Guide*; Marcel Dekker: New York, 2000; Chapter 2 pp 59–64 and Chapter 3 pp 210–212.
- (43) QSense AB. *QTools Step by Step*, users' manual for QCM; Gothenburg: Sweden, 2006.
- (44) Khire, V. S.; Lee, T. Y.; Bowman, C. N. *Macromolecules* **2008**, *41*, 7440–7447.
- (45) Connal, L. A.; Kinnane, C. R.; Zelikin, A. N.; Caruso, F. *Chem. Mater.* **2009**, *21*, 576–578.
- (46) Hoyle, C. E.; Lowe, A. B.; Bowman, C. N. *Chem. Soc. Rev.* **2010**, *39*, 1355–1387.
- (47) Khire, V. S.; Lee, T. Y.; Bowman, C. N. *Macromolecules* **2007**, *40*, 5669–5677.
- (48) Lowe, A. B. *Polym. Chem.* **2010**, *1*, 17–36.
- (49) Qiu, X.-P.; Winnik, F. M. *Macromol. Rapid Commun.* **2006**, *27*, 1648–1653.
- (50) Uygun, M.; Tasdelen, M. A.; Yagci, Y. *Macromol. Chem. Phys.* **2010**, *211*, 103–110.
- (51) Kade, M. J.; Burke, D. J.; Hawker, C. J. *J. Polym. Sci., Part A: Polym. Chem.* **2010**, *48*, 743–750.
- (52) Johnson, E. C. B.; Kent, S. B. H. *J. Am. Chem. Soc.* **2006**, *128*, 6640–6646.